

Seasonal footprints on ecological time series and jumps in dynamic states of protein configurations from a nonlinear forecasting method characterization

Leonardo Reyes^{1,*}, Kilver Campos², Gilberto D. Avendaño², Lenin González-Paz³, Alejandro Vivas³, Ysaías J. Alvarado⁴, and Saúl Flores⁵

¹Laboratorio de Dinámica no-lineal y Sistemas Complejos, Centro de Física, Instituto Venezolano de Investigaciones Científicas (IVIC), República Bolivariana de Venezuela.

²Laboratorio de Física de Fluidos y Plasmas, Centro de Física, Instituto Venezolano de Investigaciones Científicas (IVIC), República Bolivariana de Venezuela.

³Laboratorio de Biocomputación. Centro de Biomedicina Molecular. Instituto Venezolano de Investigaciones Científicas (IVIC). Maracaibo, Edo Zulia, República Bolivariana de Venezuela.

⁴Laboratorio de Química Biofísica Teórica y Experimental. Centro de Biomedicina Molecular. Instituto Venezolano de Investigaciones Científicas (IVIC). Maracaibo, Edo Zulia, República Bolivariana de Venezuela.

⁵Laboratorio Ecología de Suelos, Centro de Ecología, Instituto Venezolano de Investigaciones Científicas (IVIC), República Bolivariana de Venezuela.

* corresponding author: leonardoivanrc@gmail.com

October 10, 2024

Abstract

We have analyzed phenology data and jumps in protein configurations with the nonlinear forecasting method proposed by May and Sugihara. Full plots of prediction quality as a function of dimensionality and forecasting time give fast and valuable information about Complex Systems dynamics. At the end of this second version of this manuscript we added another figure in which we consider the stationarity of the phenology data and include some additional comments regarding dimensionality.

The notion of *prediction* is at the heart of the scientific method [1] and of some theories about the mind (the predictive brain) [2]. In this article we explore decades of ecological data [3] and data from a model for sampling protein configurations using a dynamic indicator $\rho(E, T_p)$ introduced some time ago by May and Sugihara to distinguishing chaos from noise in time series [1]: ρ^2 is a number in the unit interval which quantify the quality of the predictions made by the forecasting method introduced by the authors. We have obtained valuable insights about such data when considering full plots of the quantity $\rho^2(E, T_p)$:

we are not trying to make predictions about not already measured quantities, rather we are characterizing the dynamic state of the system with the method of reference [1]. Here E is a dimensionality parameter: in the forecasting method is the number of components of vectors constructed with the data. We make a prediction T_p time steps into the *future* and the evaluation of that prediction is made with the quantity ρ by comparing predictions with actual observed values. Characterizing the dynamics of a system is a basic goal in today's big data dominated scientific practice. In this work we have applied the method proposed by May and Sugihara to analyze data spanning decades of population dynamics of several species from a Venezuelan forest [3] and to analyze some aspects of protein dynamics [9].

Given some data series x_n the nonlinear forecasting model considers vectors of E components of the form $(x_i, x_{i-1}, x_{i-2}, \dots, x_{i-(E-1)})$ and constructs a prediction for the next x_{i+T_p} value in the series; the prediction's quality is quantified with the correlation ρ between observed and predicted values. Thus, for given data x_n , the quantity $\rho(E, T_p)$ is the basic output of the method [1].

In figure 1 we show $\rho^2(T_p)$ for *Hieronyma moritzi*

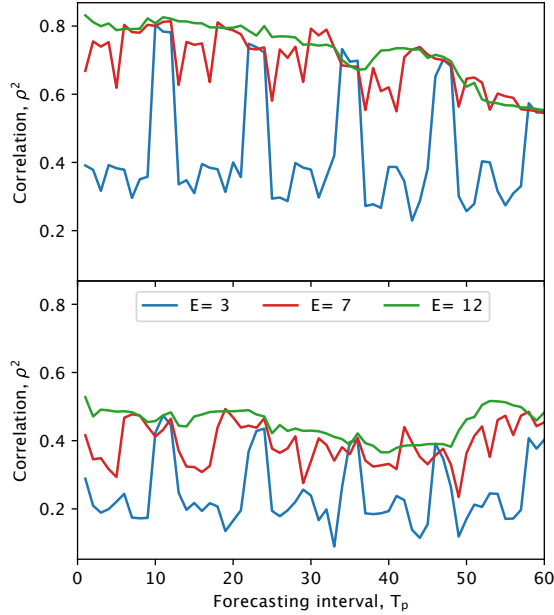


Figure 1: $\rho^2(T_p)$ for $E = 3$, $E = 7$ and $E = 12$ (*Hieronyma moritziana*). For $E = 3$ we get seasonal scales from the signal. For $E = 12$ we have that ρ decays with T_p , with T_p given in months. $E = 7$ is the first case outside the *small dimensionality* region in parameter space for this species.

Pax & *K. Hoffm* species for three values of the dimensionality parameter E , $E = 3$, $E = 7$ and $E = 12$, for signals of flowers and fruits populations as a function of time [3]. It can be appreciated that the seasonal time scale (one year) manifests itself at $E = 3$, where we obtain a periodic pattern. For $E = 12$ there is a decay in prediction quality as T_p increases [1].

Full plots of $\rho(E, T_p)$ can be very informative about the dynamic state of a system. In figure 2 we show $\rho(E, T_p)$ for *Hieronyma moritziana* species, and some features emerge: only for $E < 7$ the seasonal scale appears, and there are triangular patterns that repeat themselves each 12 months. For flowers and $E > 12$ we obtain a decay in ρ with increasing T_p . Other species have no structure in parameter space (like figure 5) or some distorted triangular patterns, see figure 3 where we show $\rho^2(E, T_p)$ for three species.

For comparison and reference we show in figure 4 (left) $\rho^2(E, T_p)$ plots for chaotic time series with different Lyapunov exponents [5]. It can be appreciated that the intersection points on the E and T_p axes are the same, and that the larger the Lyapunov exponent the smaller those intersection points. Similar triangular patterns were obtained for *Hieronyma moritziana* like species [3] but with a major difference (see figure 2): for several species we have

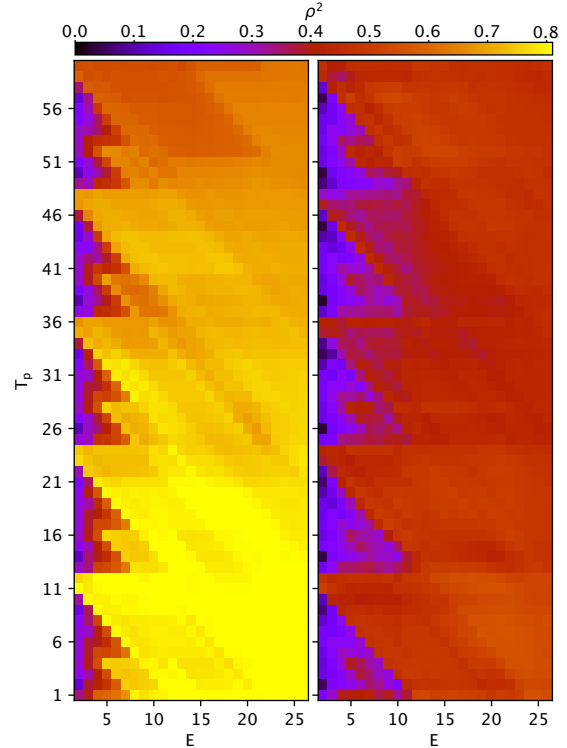


Figure 2: $\rho^2(E, T_p)$ for *Hieronyma moritziana* species: flowers (left) and fruits (right).

obtained a kind of inversion and repetition of the triangular patterns obtained for chaotic series, which prompts the question: how can we obtain low prediction quality at short times and high prediction quality at longer times?. We have found that a random decay process with resinsertion [4] produces the same kind of triangular patterns obtained for *Hieronyma moritziana* like species, this result is shown in figure 4 (right). We have generated a random decay signal with the explicit functions of González *et al*: $X_n = \sin^2(\theta\pi z^n)$, with parameter $z = p/q$, p and q being relative primes ($q > p$, $z < 1$) [5]. A random decay with reinsertion sounds very *ecosystemic* indeed. We get poor prediction at short times because it's a random process, and we obtain a high prediction quality at longer times because once the signal has decayed to near zero values the dynamic is very predictable. It can be observed in figure 2 that for *Hieronyma moritziana* and within one year we obtain a kind of superposition of two triangles (flowers mainly), corresponding to two overlapping random decay processes: wet and dry periods of the year in the Venezuelan forest [3]. A simpler plot like the one shown in figure 4 (right) highlights the underlying proposed mechanism. Since we have random decay processes of size 6, it can be said that the case $E = 7$ (see figure 1) is the smaller

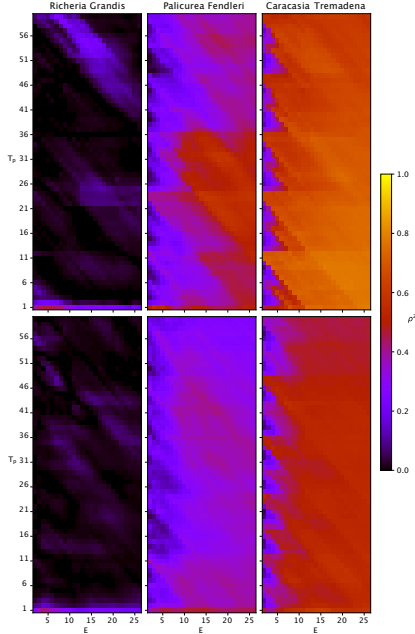


Figure 3: Three cases of population dynamics with very different predictability patterns in parameter space. Up: flowers, Bottom: fruits. See also [3].

dimensionality value E outside the *small dimensionality* region in parameter space for *Hieronyma moritziana*.

In figure 5 we have verified, with the help of the GHWS model [6], that an ideal gas type of dynamics would produce very small values of ρ^2 , for most E and T_p values. The signal used in this case was the *activity* in the system as a function of time [6, 7, 8].

In figures 6 and 7 we show a $\rho^2(E, T_p)$ plot for the atoms coordinates of a protein obtained with molecular dynamics simulations [9, 10, 11]. As an example, we have chosen a typical intrinsically disordered protein such as alpha synuclein, associated with neurodegenerative Parkinson's disease, which is known for its complex dynamic conformational behavior and tendency to form aggregates [12]. This protein is made up of three domains or regions known as the N-terminal, NAC, and C-terminal domains [13]. The signal to be processed in this case is the position of the atoms in one of the three regions of the alpha synuclein protein, for a given time. As time passes towards equilibrium the protein jumps between very different dynamic states (see figure 6): fully *disarmed* ($\rho \sim 0$ for most E and T_p), *rigid* (high values of ρ for most E and T_p), a chaotic-like structure (triangular pattern), and several more complicated $\rho(E, T_p)$ patterns. It is important to note that structural disorder has been highlighted recently for alpha synuclein wild type [14], and that we are associating predictability (large values of ρ^2) with rigidity through lost of

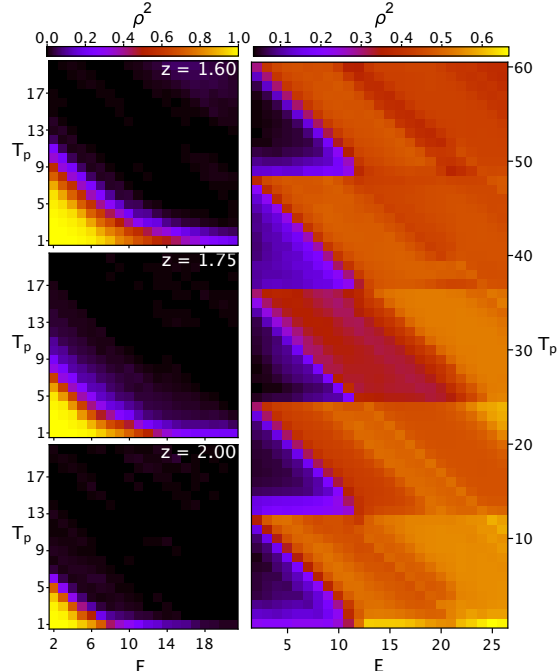


Figure 4: *left*: $\rho^2(E, T_p)$ for chaotic dynamics with different Lyapunov exponents λ . From top to bottom: $z = 1.6, 1.75, 2.0$, with $\lambda = \log z$ [5]. Similar results were obtained for the logarithmic map. *right*: $\rho^2(E, T_p)$ for synthetic data emulating a random decay process with reinsertion. We have used $z = 2/3$ in the explicit functions of references [5] for the random decay process. We used 500 data points in each case. See text.

effective degrees of freedom. A particular pattern emerges for an alpha synuclein dimer scenario: we obtain a particular dimension value E_0 for which no prediction can be made about the position of the atoms along the polymer chain, for any value of T_p , see figure 7 (left). Regarding E_0 , we have interpreted this result as implying that there are structures of length E_0 , involving E_0 number of atoms, that appear in the protein (for a given time).

So far we have shown transient protein dynamics states. In figure 7 (right) we show $\rho^2(E, T_p)$ for the N region of a mutated protein (A53T) after 100ns of simulation. The N-terminal region of the alpha synuclein protein was chosen given its important biological function of binding to the cell membrane [15, 14]. No such state were achieved for the same protein in the wild type case, and this particular dynamic state, a near equilibrium one, fits a chaotic structure scenario: good predictability for small T_p and eventually unpredictability for large T_p , but with an approximately horizontal frontier between large and near zero values of ρ^2 . These results will be further investi-

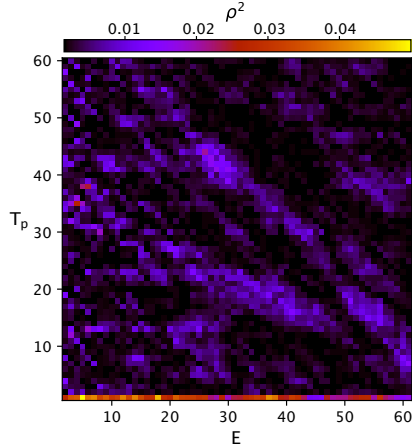


Figure 5: $\rho^2(E, T_p)$ for an ideal gas like dynamics. The processed signal was the *activity* in the system as a function of time, generated from the GHWS model [6] in a zone of parameter space that produces zero average correlations of activity (see [8], section 3.6), which results in the ideal gas equation of state [7].

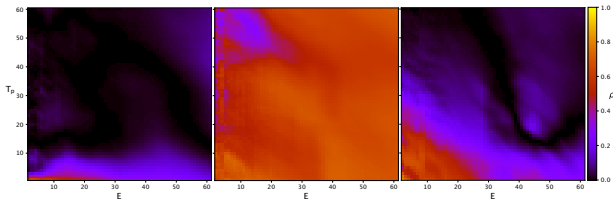


Figure 6: Protein *dynamics*, for data obtained with molecular dynamics simulations [9, 10, 11]. On the left a dynamic state, at a particular time, for which $\rho^2 \sim 0$ for most E and T_p : the protein is *disarmed*. At the center a dynamic state, at a particular time, for which ρ^2 is large for most E and T_p : the protein is *rigid*. To the right we show a chaotic like structure obtained for a particular time.

gated elsewhere, but let's consider the case of an horizontal frontier (in parameter space) between high and low values of ρ^2 . If we look at figures 1 and 2, we can see that when T_p is a multiple of 12 months ρ^2 shows a weak dependence on dimensionality E , which in turn implies that variations of ρ in parameter space (see below) points only in the T_p direction. This suggest that an approximately horizontal frontier like the one shown in figure 7 (right) could be associated with an interaction with large parts of the protein (the equivalent of *seasonal* scales in this case). Under these considerations we can say that the mutated protein gains some (pathological) rigidity because of self-interaction. Besides, it appears that this pathology could be associated to a lack of cost to make predictions, since

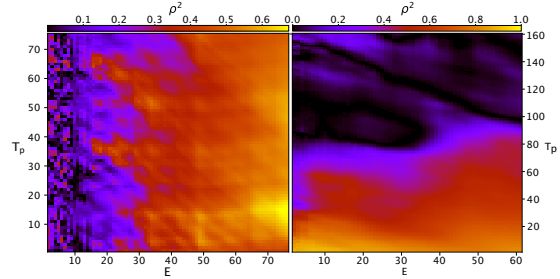


Figure 7: *left*: $\rho^2(E, T_p)$ from protein dynamics, a particular dynamic state for data obtained with molecular dynamics simulations: $\rho^2 \sim 0$ for $E = E_0 \sim 12$, for any T_p considered. *right*: $\rho^2(E, T_p)$ for α -sinuclein protein with mutation A53T, after 100ns. The input signal was the y coordinate of the atoms in the N domain.

the dimensionality parameter E can be directly related to memory capacity which certainly it is expected to have a *cost*.

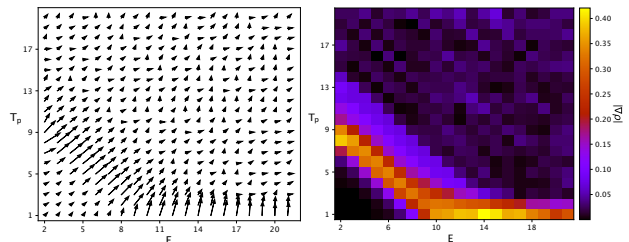


Figure 8: For data obtained from the logistic map (full chaos) we show the vector field $\nabla\rho$ (left) and the modulus of the gradient of ρ in parameter space $|\nabla\rho|$ (right). We used 500 data points. See text.

Complex adaptive systems. If we were interested in places of parameter space where *adaptation* could be done more efficiently, by changing the dynamic state of the system with minimal variation of parameters, then our ideal spots in parameter space would be places where the gradient (in parameter space) of ρ is large. As an example, in figure 8 we show the modulus and direction of $\nabla\rho$ for the logistic map. We have estimated $\nabla\rho$ from finite differences of parameters values.

From the triangular patterns found for *Hieronyma moritziana* like species in the case of phenology (figure 2) and for chaotic dynamics (figure 4 (left)) it is clear that lines of slope -1 play a role in parameter space (E, T_p). The relation $T_p = E - 1$ is significant in the method introduced by May and Sugihara: it limits the amount of information that in principle could be found in vectors of the form $(x_i, x_{i-1}, x_{i-2}, \dots, x_{i-(E-1)})$ when trying to make a prediction about x_{i+T_p} . The lines of slope -1

are perpendicular to lines of the form $T_p = E - 1$, which suggests that $\nabla\rho$ (see figure 8) is very relevant in this method, which also highlights the natural framework it provides for considering *adaptation* in Complex Systems, as commented in the previous paragraph.

We have presented results for several types of system-dynamics based on the forecasting method introduced by May and Sugihara [1]. Our results highlight the powerfulness of full plots of $\rho(E, T_p)$ obtained with the nonlinear forecasting method to analyze and characterize the dynamics of Complex Systems, for *scales* as large as forest Ecosystems and as small as Proteins.

Data availability: Data available in Zenodo at <https://doi.org/10.5281/zenodo.12610823>. Also, for more ecology data: <https://doi.org/10.5281/zenodo.7662623> (see reference [3]).

References

- [1] Sugihara G. and May R. M., Nonlinear forecasting as a way of distinguishing chaos from measurement error in time series, *Nature* **344**, 734–741 (1990).
- [2] Bubic A., von Cramon D. Y. , Schubotz R. I., Prediction, cognition and the brain, *Frontiers in Human Neuroscience* **4**, Article 25 (2010).
- [3] Flores S., Forister M. L., Sulbaran H., Díaz R. , Dyer L. A., Extreme drought disrupts plant phenology: Insights from 35 years of cloud forest data in Venezuela, *Ecology* **104**, Issue 5, e4012 (2023).
- [4] Schuster H. G. , *Deterministic Chaos: An Introduction* (Fourth edition), Wiley-VCH, 2005. See Chapter 5, fig. 58.
- [5] González J. A. , Carvalho L. B. , Analytical Solutions to Multivalued Maps, *Mod. Phys. Lett. B* **11**, 521 (1997); González J. A. , Reyes L. I. , Guerrero L. E. , Exact solutions to chaotic and stochastic systems, *Chaos* **11**, 1 (2001).
- [6] Reyes L, Laroze D., Cellular Automata for excitable media on a Complex Network: The effect of network disorder in the collective dynamics, *Physica A* **588**, 126552 (2022).
- [7] Parameter values for the GHWS model in figure 5: $K = 6$, $\sigma = 2.4$, $z = 5$, $N = 1000$. After $T = 1000$ steps we got the fluctuations in activity from the next 1000 steps. For these parameter values the normalized fluctuations $\varsigma = N(\langle F^2 \rangle - \langle F \rangle^2) / [\langle F \rangle(1 - \langle F \rangle)]$ are ≈ 1 , where F is the activity [6]. $\varsigma \approx 1$ is equivalent to say that the dynamics is an ideal gas like one (see [8], section 3.6).
- [8] Chandler D., *Introduction To Modern Statistical Mechanics*, Oxford University Press, 1987.
- [9] González-Paz L. *et al.*, Structural deformability induced in proteins of potential interest associated with COVID-19 by binding of homologues present in ivermectin: Comparative study based in elastic networks models, *Journal of Molecular Liquids* **340**, 117284 (2021).
- [10] Haliloglu T., Bahar I. , Erman B., Gaussian Dynamics of Folded Proteins, *Physical Review Letters* **79**, Number 16, 3090 (1997); Bahar I., Atilgan A. R., Erman B., Direct evaluation of thermal fluctuations in proteins using a single-parameter harmonic potential, *Folding & Design* **2** (3), 173–181 (1997).
- [11] GROMACS: [https://www.softxjournal.com/article/S2352-7110\(15\)00005-9/fulltext](https://www.softxjournal.com/article/S2352-7110(15)00005-9/fulltext)

WebGRO for Macromolecular Simulations: <https://simlab.uams.edu/>
- [12] Mehra S., Sahay S., Maji S. K., α -Synuclein misfolding and aggregation: Implications in Parkinson’s disease pathogenesis, *Biochim Biophys Acta Proteins Proteom* **1867** (10), 890-908 (2019).
- [13] Alza N. P., Iglesias P. A., Conde M. A., Uranga R. M., Salvador G. A., Lipids at the Crossroad of α -Synuclein Function and Dysfunction: Biological and Pathological Implications, *Frontiers in Cellular Neuroscience* **13**, 175 (2019).
- [14] Ray S. *et al.*, α -Synuclein aggregation nucleates through liquid–liquid phase separation, *Nature Chemistry* **12**, 705 – 716 (2020).
- [15] Fusco G. *et al.*, Direct observation of the three regions in α -synuclein that determine its membrane-bound behaviour, *Nature Communications* **5**, 3827 (2014).

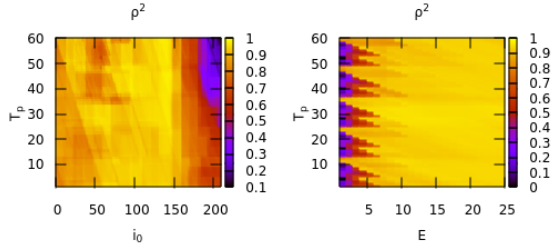


Figure 9: *left*: ρ^2 for *Hieronyma moritziana* (flowers), for high dimensionality ($E = 12$), and for windows of data of size $M = N/2$ that starts at position i_0 . *right*: $\rho^2(E, T_p)$ for *Hieronyma moritziana* (flowers) and for the first 320 points of the data set.

Now we consider new results for phenology data. Previously, for all the figures related to the Altos the Pipe ecosystem (figures (1), (2) and (3)), it was considered the full data set for each species, with $N = 420$ for *Hieronyma moritziana* species (flowers) for example, with N being the number of monthly points in the data set. In figure (9) (left) we consider windows of data of size M that start at i_0 . For example: to consider the first half of the data is to consider $M = N/2$ and $i_0 = 0$, to consider the second half of the data is to consider $M = N/2$ and $i_0 = N/2$. In figure (9) (left) it is shown $\rho^2(i_0, T_p)$ for $M = N/2$, for high dimensionality ($E = 12$), and for *Hieronyma moritziana* (flowers). It can be observed that there was a qualitative change in the dynamics as measured by ρ^2 . Early in the data the high dimensionality region virtually do not depends neither on E nor on T_p , apart from fluctuations. This is a zone characterized, as was previously stated, by a random decay process plus a random reijection, which predicts no dependence of ρ on T_p , so previously it only predicted well the small dimensionality region. By the end of the data, for large i_0 , we have a high dimensionality region in which ρ decays with T_p . An abrupt change appears for $i_0 \sim 150$ in figure (9). The smaller size of the window M the best localization of the transition point, in principle, but for smaller M he have also poorer statistics for ρ . For small dimensionality and for other similar species the same behaviour is observed. We think that the random part of the reinjection process proposed before should be relaxed in order to explain the new dynamic scenario observed by the end of the data. In figure (9) (right) we can see a new version of figure (2) in which we used only the first 320 points of the data set, in fact no dependence of ρ on T_p is observed: the decay of ρ with T_p for large dimensionality observed in figure (2) was the combination of two different dynamic regimes.

We have found that what defines the frontier between

small and large dimensionality is associated to an *overfitting* scenario, and also to the *size*, which is 6, of the random decay process. An *overfitting* could be responsible for the absence of the one year time scale for $E > 6$.